

## PARAMETRIC STUDY OF VARIABLES AFFECTING THE INTERNAL BALLISTIC ON STAR PROPELLANT GRAIN

Bagus H. Jihad

Rocket Technology Center, National Institute of Aeronautics and Space - LAPAN

[baguserek@gmail.com](mailto:baguserek@gmail.com)

### Abstract

The physical phenomena which govern the overall efficiency of a solid rocket motor are quite numerous and complex. For this reason the prediction of solid rocket motor delivered performance has, historically, been empirically oriented. Total reliance on correlations of firing data is undesirable, however, as their ranges of applicability cannot usually be clearly defined, and a priori performance predictions for new motor designs or propellants cannot be made with confidence. In order to achieve the desired generality, performance predictions should, where possible, be based on physically realistic models of the controlling phenomena. Parametric study is conducted to know the variables affect on star propellant grains for internal ballistic evaluation on solid rocket motor. An infinite number of possibilities exist. Accurate calculation of grain geometrical properties plays a vital role in performance prediction. Initial geometry is defined in the form of a surface which defines the grain configuration. Grain burn back is achieved by making new surfaces at each web increment and calculating geometrical properties at each step. In this paper, internal ballistics, and grain design, solid rocket motor performance analysis and prediction will be covered.

**Keywords:** Solid propellant grain, ballistic evaluation, star port propellant grains, burning rate, ballistic evaluation motor.

### Nomenclature

$a$	: burning rate constant	$I_{sp}$	: specific impulse (s)
$n$	: burning rate exponential	$I_t$	: total impulse (Kgf.s)
$A_b$	: burning area ( $\text{mm}^2$ )	$\dot{m}_b$	: burning mass flow rate (kg/s)
$A_e$	: nozzle exit area ( $\text{mm}^2$ )	$\dot{m}_t$	: throat mass flow rate (Kgf/s)
$A_t$	: nozzle throat area ( $\text{mm}^2$ )	$P_{amb}$	: ambient pressure ( $\text{kg/cm}^2$ )
$C^*$	: characteristic velocity	$P_c$	: chamber pressure ( $\text{Kgf/cm}^2$ )
$C_f$	: thrust coefficient	$P_e$	: exit pressure ( $\text{Kgf/cm}^2$ )
$F$	: thrust (Kgf)	$r_b$	: burning rate (cm/s)
$g_0$	: specific gravity	$\rho_b$	: propellant density ( $\text{g/cm}^3$ )
		$\gamma$	: heat capacity ratio

### 1. Introduction

Design of a solid propellant grain was governed by ballistic, processing, and structural integrity requirements. Solid propellant burning surface recedes in the direction normal to the surface at any point of time and rate of propellant consumption depends on the initial burning surface and restricted boundary. Pressure-time, thrust-time, acceleration, velocity, and trajectory are decided by propellant configuration, and are largely a geometric consideration. In the design or analysis of a solid rocket motor (SRM), one of the fundamental parameters is that of the motor chamber pressure ( $P_c$ ). For example, prediction of the chamber pressure is necessary for structural sizing the motor casing. The grain design for a solid propellant rocket motor frequently necessitates compromises among the conflicting requirements of ballistic performance, structural integrity, mission reliability, and geometrical constraints.

Among the parameters controlling the solid rocket motor operation, burning rate plays a very important role. The burning rate determines, with the burning area, the combustion processes, the mass flow rate, and therefore directly controls the pressure and thrust of the motor. Burning rate is a characteristic of the propellant that can be measured independently, at least for the more usual combustion regimes.

Accuracy of solid rocket thrust-time prediction has become increasingly more important in solid rocket design. One of the most significant variables in this prediction is the propellant burning rate. Accuracy of this value depends on empirical methods for calculating burning rate. Thrust is very sensitive to the reference propellant burning rate. Design and operation of solid rocket motors strongly depend on the combustion features of the propellant charge (burning rate, burning surface, and grain geometry) and their evolution in time. *Internal ballistics* is the applied science devoted to these problems.

For such small batches, physical (density), chemical (combustion gases properties), mechanical (tensile strength, percentage elongation, modulus) and ballistic (specific impulse, burning rate, characteristic velocity) properties of the products are determined and matched with pre-specified values. Ballistic evaluation motor (BEM) is very popular for such assessments, especially for the evaluation of ballistic properties. These give an insight into the burning rate of propellant at various operating temperatures and pressure ranges.

During the initial phase of design of solid propellant rocket motors it is necessary to identify and quantitatively estimate deviation of internal ballistics parameters of observed rocket motors types from ideal conditions. In an initial stage of the design of real rocket motors there are differences between the rocket motor theoretical performances and actual performances based on testing of standard ballistic motors.

Studying deviations that occur due to changes in internal ballistic variable is the purpose of this paper. This paper presents about the existing propellant configurations, parametric studies on star port propellant grains on a 200mm rocket motor.

## 2. Internal Ballistics

In a solid rocket motor, hot gases generated by the chemical reaction between a fuel and an oxidizer stored within the motor are accelerated to supersonic velocities through a nozzle designed to develop the resultant force. Propulsion thus is achieved by the conversion of the thermal energy of a chemical reaction into the kinetic energy of combustion products. The effectiveness of this process is predicted and assessed by evaluating the reaction thrust developed through the pressure imparted momentum of the expanded exhaust gases.

Ballistic design includes designing and modeling the internal geometry of the solid rocket motor propellant, or grain. The geometry directly affects pressure and thrust profiles and defines the amount of internal case surface exposed to hot combustion gases during motor operation.

Thus, the thrust developed is dependent on exhaust product mass flow rate, nozzle exit exhaust velocity and pressure, ambient pressure, and nozzle exit area. In turn, the initial three parameters are dependent on propellant and motor characteristics that may include propellant burning rate, density, burning-surface area and progression, combustion chamber pressure and gas temperature, and various geometric characteristics of the nozzle. Other variables (e.g., specific impulse and thrust coefficient) often used to evaluate or compare the performance of rocket motors are highly dependent on these initial three parameters<sup>4</sup>.

In the simulation of solid propellant combustion, combustion chamber pressure is a function of the mass burning rate of propellants (depending on the burning area, burning rate and density of propellants) and the mass outflow rate of combustion products through the critical nozzle section (function of pressure in the combustion chamber and the throat area and the coefficient of the mass flow rate)<sup>5</sup>.

The propellant burn rate follows the relationship<sup>10</sup>,

$$r_b = a(P_c)^n \quad (1)$$

where  $a$  and  $n$  are empirical constants, which are ideally constant over wide pressure range. This reveals that the burn rate of the propellant is directly related to the internal pressure of the motor. Some manipulation is required to determine pressure at each webstep. The mass flux of the grain is found using

$$\dot{m}_b = \dot{r}_b \rho_b A_b \quad (2)$$

The mass flow through the throat is defined by

$$\dot{m}_t = \frac{P_c A_t}{C^*} \quad (3)$$

If it is assumed that steady-state conditions exist then

$$\dot{m}_b = \dot{m}_t$$

This assumption is valid except during motor startup and tail-off where transient effects become significant, however in most cases this causes only negligible error in the results. It can be shown after some manipulation that<sup>10</sup>.

$$P_c = \left[ \frac{a A_b \rho_b C^*}{A_t} \right]^{\frac{1}{1-n}} \quad (4)$$

It is clear that pressure is a function of the burn area,  $A_b$ . The burn rate,  $r_b$ , is determined from the pressure using Eq. (2). Time is then found by dividing the webstep (arbitrarily defined) by the burn rate. This method correlates  $A_b$ -webstep profile to the pressure-time profile and illuminates why the profiles are similar.

There are several parameters used to measure motor performance. The ones used here are total impulse, specific impulse, internal motor pressure, thrust, and burn time. Total impulse (Kgf-s) is defined as NASA 8076

$$I_t = \int F \cdot dt \quad (5)$$

Specific impuls (s) is defined by

$$I_{sp} = \frac{\int F dt}{g_o \int m dt} = \frac{I_t}{g_o \int m dt} \tag{6}$$

where  $g_o$  is standard acceleration of gravity. Its units are simplified to seconds though specific impulse does not refer to time. The units are accurately defined as thrust per unit weight flow rate, or Newtons-seconds per go-(kilogram/second)-seconds Internal motor pressure is calculated as previously discussed. Thrust is determined from

$$F = C_F A_t P_c \tag{7}$$

Where

$$C_F = \sqrt{\frac{2\gamma^2}{\gamma-1} \left[ \frac{2}{\gamma+1} \right]^{\frac{\gamma+1}{\gamma-1}} \left[ 1 - \left[ \frac{P_e}{P_c} \right]^{\frac{\gamma-1}{\gamma}} \right]} + \left[ \frac{P_e - P_{amb}}{P_c} \right] \frac{A_e}{A_t} \tag{8}$$

$C_F$  is a function of the ratio of specific heats,  $\gamma$ , exit, chamber, and ambient pressures, and nozzle area ratio.

### 3. Data

The propellant used in this work is a representation of typically used propellant. No attempt is made to design a propellant as this is a task more suitable for chemists or chemical engineers than for ballistics engineers. Only the solid propellant properties and gas properties are required to complete the SRM definition. Solid propellant grain with essential geometric and ballistic parameters used in this study given in Table 1. Performance prediction was done and the result shown in Table 2.

Table 1. Salient geometric and ballistic parameters of evaluated propellant

Input parameter	Data	Geometrical grain
Outer diameter of the grain (mm)	182	
Grain configuration	Star	
Number of star point	8	
Angular fraction of star (degree)	37,31	
Star half angle (degree)	22,5	
Star outer diameter (mm)	90,8	
Fillet radius (mm)	3,2	
Tip radius (mm)	6,1	
Density of the grain (Kg/cm <sup>3</sup> )	1,62	
Burning rate (mm/s)	7	
Burning rate coefficient	0,029	
Burning rate exponential	0,433	
Length of propelan (mm)	1000	
Thoat diameter (mm)	27	
Specific heat at constant pressure (J/kg-K)	1.2	

Table 2. Performance prediction

Parameter	result
Burning time, $t_b$ (s)	2,976
Max pressure, $P_c$ (Kg/cm <sup>2</sup> )	53,269
Avg pressure, $\bar{P}_c$ , (Kg/cm <sup>2</sup> )	40,592
Max Thrust, $F$ (Kgf)	1712,090
Avg Thrust, $\bar{F}$ (Kgf)	1276,927

The main goal of a star grain configuration is to add more initial surface area. Given a particular propellant formulation, the performance of a solid rocket motor is due largely to two factors: first, its volumetric efficiency and second, its average pressure over the course of the burn. Using a star design to add more initial burn area allows for greater start-up pressure and a more neutral-regressive burn; which follows the ambient pressure curve more precisely. Additionally, the star design increases volumetric efficiency; increasing total impulse. The additional initial burn area also keeps the pressure in the chamber at a constant level, which allows for a higher average pressure during the burn which increases efficiency. The star grain configuration will also increase the range of possible payloads a sounding rocket can carry.

The star could be characterized by seven independant variables, define as web thickness, star radius, tip radius, external radius, star angle, secant fillet angle and numbe of star point. The value of a star angle for neutrality is reproduced in Table 3<sup>7)</sup>. For this study 8 star was used as seen on Table 1 above.

Table 3. number of star point and star angle

N	$\eta$ (deg)	$\pi/N$ (deg)
3	24.55	60.00
4	28.22	45.00
5	31.13	36.00
6	33.53	30.00
7	35.56	25.71
8	37.31	22.50
9	38.84	20.00

#### 4. Discussion

##### 4.1. Burn Area

The parameters of burn area,  $A_b$ , and webstep are easily obtained from any preferred CAD program (AutoCAD was used here). The burn distance intervals are modeled by offsetting burning surfaces and can be arbitrarily chosen. Usually, the web is determined and is divided into approximately fifteen or more websteps<sup>3)</sup> (25 websteps was used in this study). This is heuristic and depends upon the detail required of the grain being modeled. The burn area,  $A_b$ , is then found for each webstep by using the analysis tools in the CAD program, Fig. 2.

The profile of the burn area,  $A_b$ , versus webstep plot relates to the profile the internal pressure versus time plot. In fact, the shapes are similar except during motor startup and motor tail-off (end of motor operation) where transient effects become significant. This is clear when a burn area profile is compared to a pressure profile, provided in Fig.3. Additionally, the thrust-time profile follows the pressure-time profile. This allows to custom fit a specified pressure or thrust profile by modifying the grain internal geometry while knowing nothing of the fuel.

An increase in initial burn area facilitates the minimum startup pressure requirement. However, increasing the initial burn area without sacrificing volumetric efficiency is quite a challenge. Getting the burn area to stay nearly constant or decrease slightly over the course of the burn would provide optimum performance.

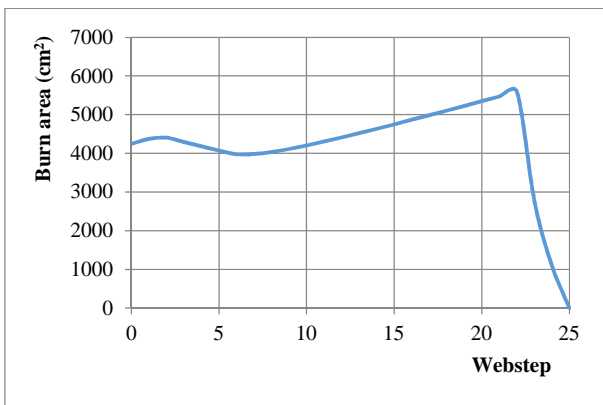


Fig. 1. Burn area profile.

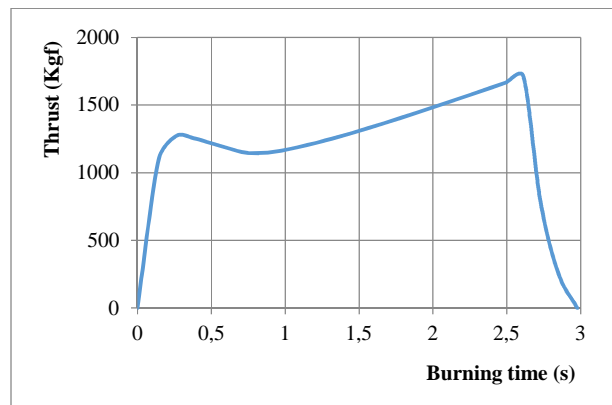


Fig. 2. Thrust vs time profile.

To assess changes in the burning area, performed simulations by varying the length of propellant. Burning area was made 90% smaller if there are inaccuracies in the size of the production or on mandril grain. Subsequently made 110% and 120% greater to anticipate if there is crack in the propellant during combustion process or when handling. Result are given on Table 4. Decreasing burning area will decrease the chamber pressure and conversely, increasing burning area will cause an increase in the chamber pressure. Reduction in burning area by 10% led to decrease of 7.25% chamber pressure and 7.9% thrust. But, increasing the burning area by 10%, then the pressure increased 10.67% and 11.67% of the thrust. Pressure and thrust profile are given in Fig. 3 and Fig. 4 respectively.

Table 4. Rocket motor performance due to changes in the burnig area.

Burn area (mm <sup>2</sup> )	Pc (Kg/cm2)	C <sub>f</sub>	F (Kgf)	t <sub>b</sub> (s)
0,9 A <sub>b</sub>	47,49785	1,543051	1510,686	3,000
A <sub>b</sub>	51,21152	1,553785	1640,131	2,976
1,1 A <sub>b</sub>	56,67546	1,567916	1831,630	2,954
1,2 A <sub>b</sub>	62,18235	1,580526	2025,763	2,933

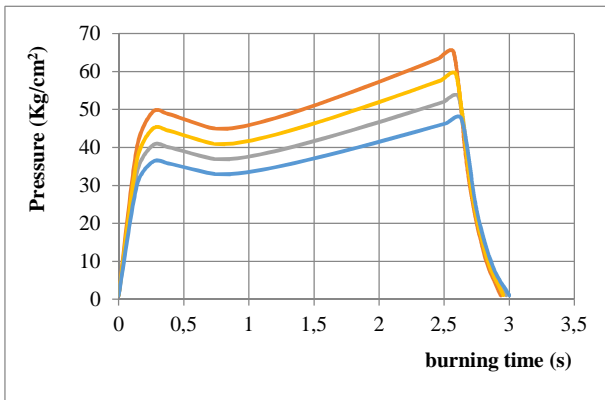


Fig. 3. Pressure changes due to burn area.

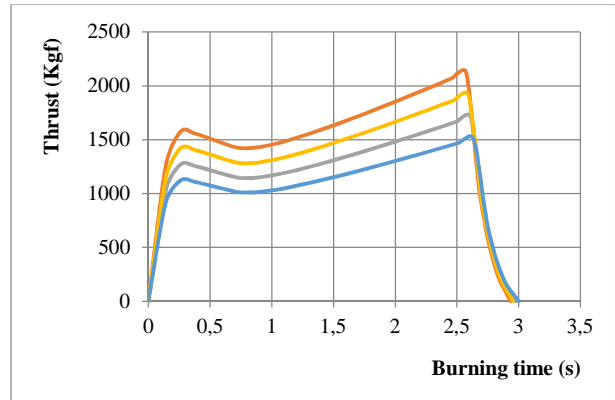


Fig. 4. Thrust changes due to burn area.

#### 4.2. Burn Rate Variation

Knowing burning rates of solid propellants, whether steady or unsteady, under a variety of operating conditions is of critical importance both for applications (due to their sensible influence on performances and cost of propulsive devices) and fundamental reasons (understanding of combustion processes).

Furthermore, since no available theory/model is capable of predicting burning rates with accuracies within 1 % and including the effects of rate modifiers, they must be measured experimentally<sup>5</sup>. In general, burning rates depend on nature of energetic material (basic ingredients and their mixture ratio); details of chemical composition (catalysts, modifiers, additives, etc. usually present in small or fractional percentages); physical effects (particle size distribution, presence of wires or staples, etc.); details of manufacturing process and other miscellaneous factors; operating conditions (pressure, initial temperature, natural and/or external radiation, heat losses, gas flow parallel to the burning surface, acceleration, etc.); mode of operation (steady vs. unsteady).

To observe the change in the performance of the rocket motor, then the value of the burn rate was increased from 0.7 to 0.75 and 0.8. The result are given on Table 5 and Fig. 5 and Fig. 6. Increasing burning rate about 7% increase the chamber pressure 6% and 6,87% of thrust. Increasing burning rate about 14,25% will increase 12,56% of pressure and 13,73% of thrust.

Table 5. rocket motor performance due to changes in burning rate.

Burning rate (cm/dt)	Pc (Kg/cm <sup>3</sup> )	C <sub>f</sub>	F (Kgf)	t <sub>b</sub> (s)
Initial	53,26868	1,55932	1712,090	2,976
0,75	56,61868	1,56778	1829,634	2,796
0,8	59,95891	1,57561	1947,252	2,638

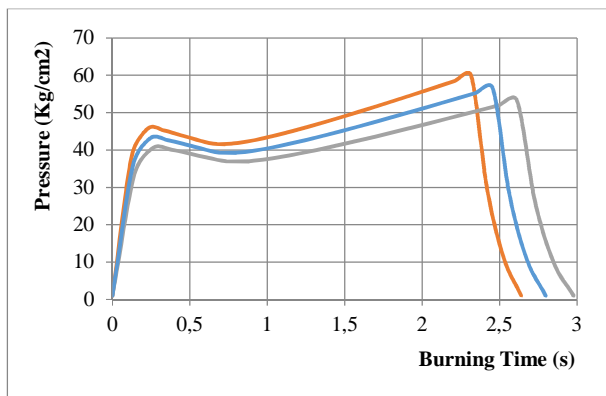


Fig. 5. Pressure changes due to burning rate

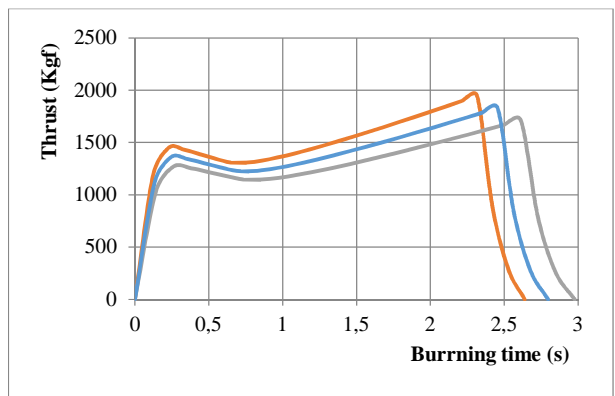


Fig. 6. Thrust changes due to burning rate

### 4.3. Density of The Propellant

Thrust and impulse are direct functions of the flow rate of the mass being discharged by a rocket motor. For accurate performance predictions, the density of the propellant generating this discharging mass must be known. Propellant density is determined from samples of the propellant being used in the motor design.

Density of the propellant composition is assumed to change from 1.62 g/cc to 1.68 g/cc and pressure time and thrust time profile for each case is plotted on the same scale as shown in Fig. 7 and Fig. 8, respectively and on Table 6. It is clear that at lower density, pressure realized for the same configuration is lower. In this case, both neutral as well as peak pressure is lowered with minor increase in the burning duration. But neither the neutrality factor is affected nor the tail-off factor, it's has any variation. It is observed that tail-off duration reduces with rise in density but corresponding rise in total burning time neutralizes the effect. Higher density ensures higher propellant weight also.

Although density of propellant formulations do not change significantly, and on the other hand, changing density of realized formulation with similar ballistic, mechanical, and other qualitative requirements is difficult to implement.

Table 6. Performance due to changes in propellant density.

Density (Kg/cm <sup>3</sup> )	P <sub>c</sub> (Kg/cm <sup>2</sup> )	C <sub>f</sub>	F (Kgf)	t <sub>b</sub> (s)
1,62	53,26868	1,559319	1712,090	2,976
1,64	53,98622	1,561186	1737,230	2,973
1,66	54,70486	1,563025	1762,429	2,970
1,68	55,42459	1,564836	1787,686	2,967

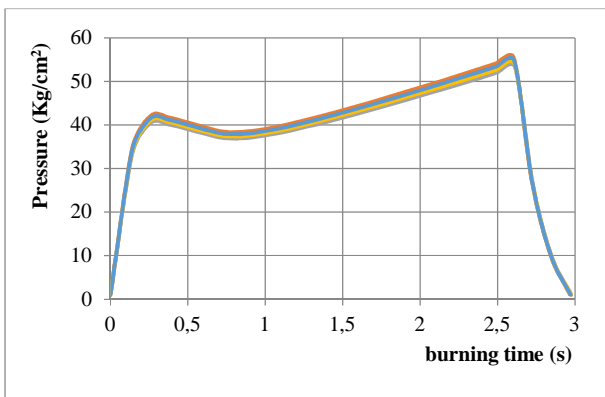


Fig. 7. Pressure changes due to density.

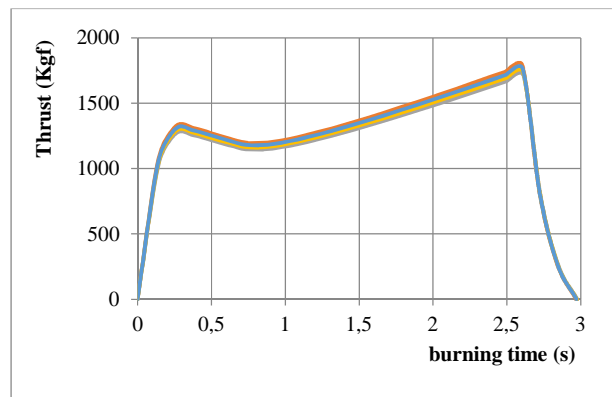


Fig. 8. Thrust changes due to density.

### 4.4. Thrust Coefficient

The nozzle characteristics that most influence motor propulsion performance are throat area  $A_t$ , and thrust coefficient  $C_F$ . Ideally, thrust coefficient, defined as  $C_F = F/P_c \cdot A_t$ , [Eq. (7) and Eq.(8)] is a function only of nozzle geometry; gas specific heat ratio; and chamber, ambient, and nozzle exit pressures. In actual systems, however, this nozzle performance coefficient is influenced also by the two phaselag chemical nonequilibrium, boundary layer losses, and transfer or heat to the nozzle. Typical maximum values of performance losses for the first three are 5 percent two phase lag, 2 percent become recombination and 2 percent viscous losses. Heat loss to the nozzle is very dependent on the heat sink properties of the nozzle material and the motor firing duration; no typical maximum percentage loss can be indicated, predicting these loss factors necessitates combining theoretical analysis with empirical relationship and demonstrated performance.

The degree to which the thrust is amplified by the nozzle is quantified by the Thrust Coefficient ( $C_F$ ), and is defined in terms of the chamber pressure and throat area. A well designed nozzle will deliver a  $C_F$  of about 1.5 under steady-state conditions. Ideal  $C_F$  for the same nozzle would be around 1.65<sup>(6)</sup>. Thrust coefficient and performance prediction are given in Table 7. Study conducted by changing the throat area of the nozzle from 27 mm to 30 mm with an increase about 1 mm radius. Although this change is very small, but it can reduce a significant pressure, see Fig. 10.

However, changes in thrust coefficient can happen even with the same throat area for several reasons. The losses which affect the thrust coefficient include divergence of the flow at exit from the nozzle, skin friction losses within the nozzle, and two-phase flow. In addition the thrust may be reduced because the flow area at the throat is less than the geometric area due to throat curvature and the presence of the boundary layer<sup>(6)</sup>.

Table 7. Rocket motor performance due to changes in throat area

Throat radius (cm)	$P_c$ (Kg/cm <sup>2</sup> )	$C_f$	F (Kgf)	$t_b$ (s)
2,7	53,26868	1,55932	1712,090	2,976
2,8	49,21247	1,54813	1688,854	2,992
2,9	45,60001	1,53715	1666,745	3,008
3	42,36912	1,52635	1645,655	3,022

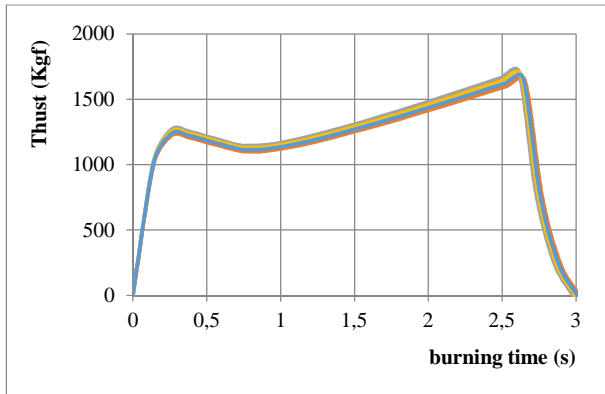


Fig. 9. Pressure changes due to throat area.

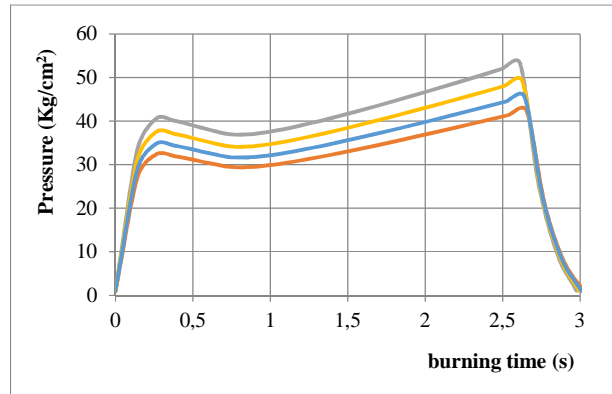


Fig. 10. Thrust changes due to throat area.

LAPAN motor firings have indicated that metal oxide is deposited on the nozzle throat surfaces during portions of a motor firing, especially for a small motor. When these deposits build up, it can reduce the throat area enough to produce an increase in the chamber pressure. These deposits are discharged either when the nozzle surface temperature attains the melting temperature of the metal oxide or when the gas dynamic drag forces exceed the strength of the deposit.

If the breakdown of the deposit depends primarily on surface temperature, the buildup occurs once in the early phases of firing. If the breakdown depends primarily on drag forces, the deposits may form repeatedly. In either case, performance is affected. However, while the deposit studies have been informative and have identified a possibly significant phenomenon, they have not produced analytical techniques currently accepted for use in predicting the occurrence and buildup of these deposits.

### 5. Conclusion

No performance prediction methodology would be complete without considering such effects as burn rate, nozzle erosion and particle size. All the variables discussed are always associated with pressure. Rocket motor designer must consider the maximum pressure requirement. If the pressure is too high, the pressure vessel could crack or break resulting in total mission failure.

Values of average thrust and pressure are necessary in the initial estimate of nozzle throat area. These averages may be treated as the average over burning time or action time; therefore, the values stipulated or derived are sufficient. With respect to grain configuration and propellant burning rate, however, the time necessary to burn the propellant web is of principal concern. The grain design should be considered complete only when the required performance is substantiated by appropriate performance prediction and analysis and the grain is deemed structurally adequate.

There are still many things that need to be studied to gain a comprehensive understanding of internal ballistics. Some aspects or variables that are discussed related to another variable that assumed constant.

### References

- 1) Shekhar, Himanshu, *Design of Funnel Port Tubular Propellant Grain for Neutral Burning Profile in Rockets*, Defence Science Journal, Vol. 59, No. 5, September 2009, pp. 494-498
- 2) Fry, Ronald. S, *Solid Propellant Subscale Burning Rate Analysis Methods For U.S. And Selected Nato Facilities*, CPTR 75, January 2002.
- 3) Moore, Stephen Scot, *Ballistics Modeling Of Combustion Heat Loss Through Chambers And Nozzles Of Solid Rocket Motors*, Thesis in Mechanical Engineering, California State University, Sacramento, USA, 2010.
- 4) Anon. *Solid Rocket Motor Performance Analysis and Prediction*, NASA SP-8039, 1971.
- 5) Terzic, Jasmin., Zecevic, Berko, *Numerical Simulation of Internal Ballistics Parameters of Solid Propellant rocket Motors*, 15th Proceeding New Trends in Research of Energetic Materials, University of Pardubice, Czech Republic, 2012, Part II, pp. 881-892.

- 6) Bose P., Pandey, K. M., *Analysis of Thrust Coefficient in a Rocket Motor*, International Journal of Engineering and Advanced Technology (IJEAT), Volume-1, Issue-3, February 2012, pp 30-33
- 7) Jihad, Bagus H., *Analisis Pembakaran Propellant dengan Grain Bintang*, Presented on Seminar of JASAKIAI, April 2013, Yogyakarta, Indonesia.
- 8) Anon, *Solid Propellant Selection And Characterization*, Space Vehicle Design Criteria, NASA SP-8064, 1971.
- 9) Anon, *Solid Propellant Grain Design and Internal Ballistics*, Space Vehicle Design Criteria (Chemical Propulsion), NASA SP-8076, 1972.
- 10) Sutton, G. P. and Biblarz, O., *Rocket Propulsion Elements*, 7th ed., John Wiley and Sons, New York, 2001.